Design, fabrication and characterization of a single-layer out-of-plane electrothermal actuator for a MEMS XYZ stage

Yong-Sik Kim
National Institute of Standard and Technologies,
Intelligent System Division
100 Bureau Dr. Gaithersburg, MD, 20899, USA
1-301-975-8081
mk37do@gmail.com

Nicholas G. Dagalakis
National Institute of Standard and Technologies,
Intelligent System Division
100 Bureau Dr. Gaithersburg, MD, 20899, USA
1-301-975-5845
nicholas.dagalakis@nist.gov

Satyandra Gupta
University of Maryland,
Department of Mechanical Engineering
University of Maryland, College Park, Maryland 20742, USA
1-301-405-5306
skgupta@umd.edu

ABSTRACT

This paper presents the design, fabrication and characterization of a single-layer out-of-plane electrothermal actuator based on MEMS (Micro-Electro-Mechanical System). The proposed electrothermal actuator is designed to generate motions along the out-of-plane or normal to a wafer by a Joule heating when the current flows through the actuator. This out-of-plane electrothermal actuator is based on a single layer of a SOI (Silicon on Insulator) wafer and two notches near the middle of the actuator beams. Due to these notches, the thermal expansion of the beams in the actuator generates an eccentric loading, which converts into the bending of the beams. This bending of the beam finally generates the out-of-plane motion at the middle of the beam. This behavior is described by the prepared analytic equations and compared by the results from FEM (Finite element Model) analysis. With fabricated samples, a 30 μm displacement is measured along out-of-plane at 5 V driving voltage. The 1st mode of the resonant frequency for the out-of-plane motion is expected to occur at 74.9 kHz from FEA. The proposed actuator is based on the standard SOI-MUMPs (SOI-Multi User Manufacturing Process) , so it has good integration capability with other system employing same fabrication techniques. To test its integration capability, a MEMS XYZ stage is fabricated by embedding the proposed out-of-plane electrothermal actuator onto an existing MEMS XY stage. The range of motion of the fabricated XYZ stage is measured about 35 μm x 35 μm x 30 μm along X, Y and Z axes without any changes on its fabrication process.

Categories and Subject Descriptors

B.7.1: [Integrated Circuits]: Types and Design Styles -- advanced technologies

General Terms

Experimentation, Design

Keywords

MEMS, out-of-plane, electrothermal actuator, eccentric loading, buckling

1. INTRODUCTION

The MEMS (Micro Electro Mechanical System) based actuators have been widely used at metrology and micro-manufacturing applications such as micro confocal imaging [2, 3, 4], bio-cell manipulation [5] and nano-assembly [6], due to their accurate motion, nanometer level resolution, small footprint, system integration flexibility and tens of micron meters of motion [1].

There are some factors to consider at designing MEMS actuators; range of motion, thrust force, frequency response and integration capability with external system. The system integration capability includes the difficulty of the fabrication process. If the fabrication of the proposed system is too difficult to complete or totally different fabrication techniques are needed, its integration capability is also affected by these factors. If the proposed system doesn't need any special processes and can share with the fabrication process of the target systems, the proposed system has a reasonable integration capability with the target systems. Therefore, the integration capability is also an important factor to consider at design level when the tight interaction with other external system is required.

Among a variety of integration, a combination of in-plane actuation systems with out-of-plane actuation systems is not common. This is because the fabrication processes for the in-plane actuators are considerably different from that of the out-of-plane actuators. For out-of-plane motion, structures in height are needed, so at least two or more layers are needed to be stacked up and combined together for the out-of-plane motion as shown in bi-morph or multi-morph actuators [11, 12]. But, most in-plane actuators don't need multiple layers for their operation [8]. This structural differences cause difficulty in integration. This paper describes the design and fabrication of the out-of-plane actuator with reasonable integration capability with in-plane actuation systems.

Among various MEMS based actuators, an electrothermal actuator can generate a stronger force with a smaller footprint and a simpler design than other actuators including electrostatic actuators [7]. But, many out-of-plane electrothermal actuators reported have multi-layers forms. The bimorph electrothermal

actuator utilizes different thermal expansion coefficients between layers. When one layer is on top of the other and their ends are linked together, different thermal expansion can generate the out of plane motion [12, 13]. But the connection of parts between multi-layers tends to be under significant shear stress during operation, so those tend to fail faster than other parts and reduce the total life-time of the system. To avoid this kind of a problem, a single layer electrothermal actuator was introduced [10]. The single layer actuator is made of a single layer with different height like bridges or steps [9, 10], so there is no stress concentration between layers. With the single layer, the life-time of the proposed actuator can be protected [10]. But this step-bridge shape needs additional processes to build the desired step shapes on the single layer. This can reduce its integration capability with external applications. Another approach is to use a single-layer simple beam operating within its buckling mode. By utilizing a buckling mode, the out-of-plane motion can be achieved without a special fabrication process. But most buckling modes are bi-stable and a little bit unpredictable, so it is not easy to control the actuator at a desired position between bi-stable positions accurately [11].

This paper presents the design, fabrication and testing of an electrothermal actuator for out-of-plane motion. The proposed actuator is also made of a single layer and follows standard Silicon-On-Insulator Multi-User-Manufacturing Processes (SOI-MUMPs). With these features, the proposed actuator is expected to have easy integration with other in-plane actuators, if they are also based on the same fabrication processes (SOI-MUMPs). The proposed electrothermal actuator design consists of a single beam and two notches at both ends of the beam as shown in Figure 1(a). Due to the single layer with notches, Joule's heating of the beam generates the eccentric load, which converts into the bending moment for the out-of-plane motion. To demonstrate its integration capability, one existing XY stage is adopted and the proposed actuator is embedded into it, which follows standard SOI-MUMPs. This paper is organized as follows: An analytic expression was developed for the design of the proposed actuator with appropriate dimensions in section 2. This design was verified by finite-element-analysis (FEA) in section 3. Detail fabrication description was provided in section 4. The range of motion was measured at section 5. Easy integration with existing MEMS systems was demonstrated by building one MEMS XYZ stage with the proposed actuator in section 6. The conclusion and discussion are in section 7.

2. DESIGN AND ANALYSIS

Figure 1 illustrates the CAD design of the single layer electrothermal actuator and a close-up view near its attachment points notches (see Figure 1(b)). These are the flexure type structures necessary for implementing the out-of-plane bending motion of the actuator.

The schematic diagram of the proposed actuator beam can be represented like the one shown in Figure 1(c). When the thermal expansion occurs, the expected deformation is shown in Figure 1(d). It is clear that the thermal expansion generates the out-of-plane motion due to a bending moment. Figure 1(e) shows the free-body diagram of the beam. Due to the beam notches, the external force P can be regarded as an eccentric loading applied to the beam ends at distance e. The eccentric loading P can be replaced with the centric force P and a couple of moment M, as shown in Figure 1(f). Based on the free-body diagram in Figure 1(f), the beam differential equation can be written and solved as [14]:

(1)

— — — — (2)

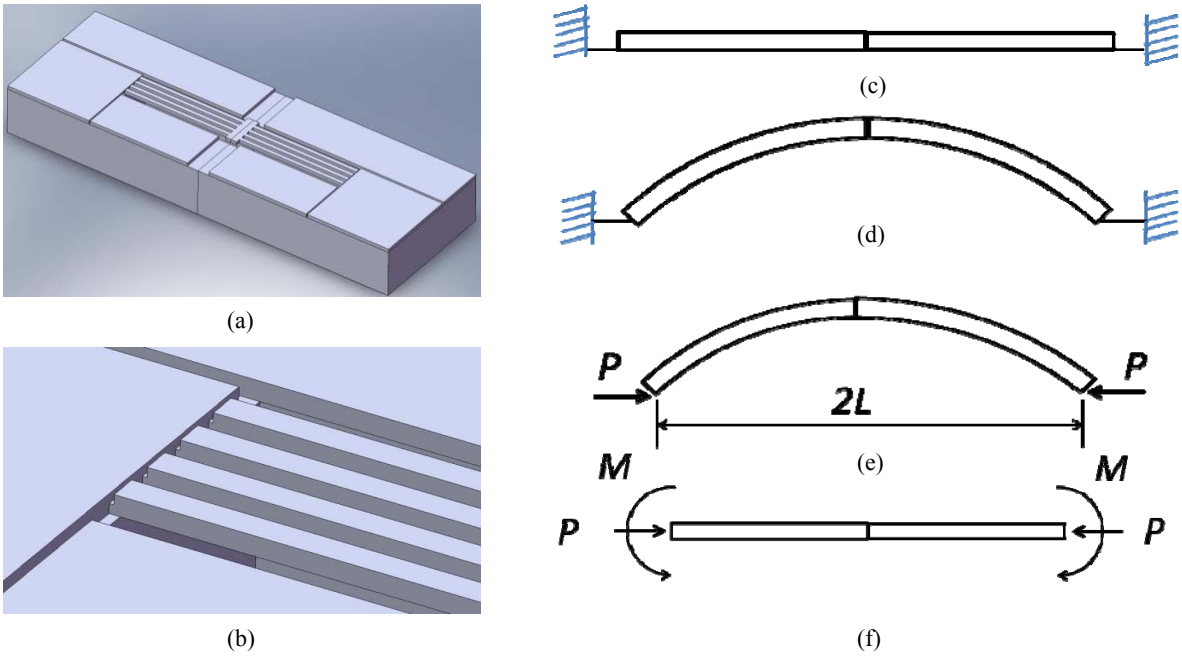

Figure 1. Schematic design of the electrothermal actuator; (a) the basic design of the electrothermal actuator for the out-of-plane motion; (b) the notch on the beam in the actuator; (c) a schematic diagram of the proposed actuator; (d) the expected deformation when the thermal expansion occurs; (e) a free-body diagram of the proposed actuator; (f) the converted free-body diagram

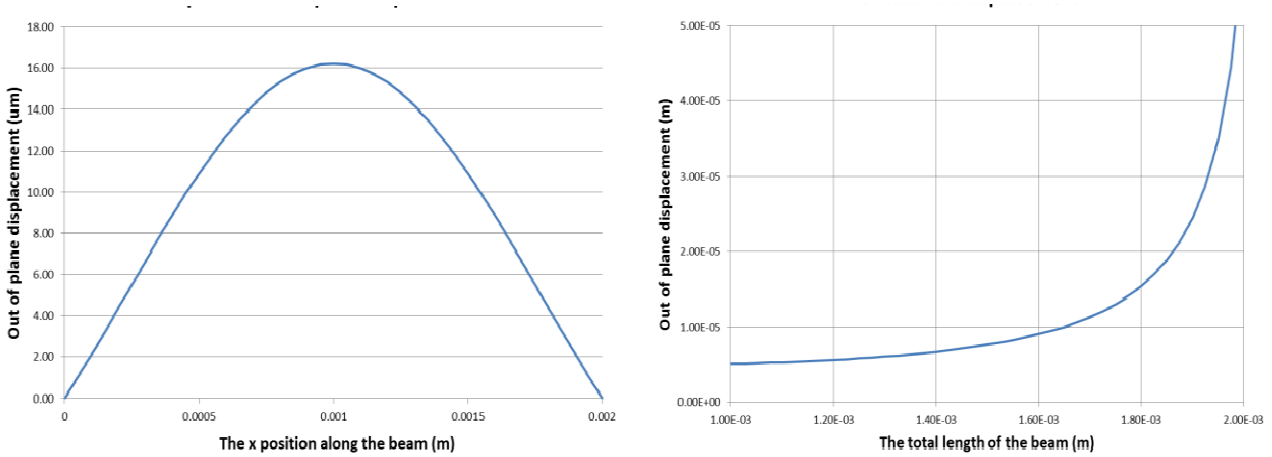

(a) (b)

Figure 2. Electrothermal actuator beam out-of-plane displacements; (a) for selected dimensions; (b) for various beam lengths

Where, E is the Young's modulus of Silicon and I is the moment of inertia. e is the distance from the center of the beam to the eccentric loading. The solution of the equation (2) with its boundary conditions (x0=0, y0=0 and x1=L, y1=0) can be given as:

(3)

The expected deformation profile of the beam for a P = 10 mN force is derived based on equation (3) and shown in Figure 2(a).

(4)

From equation (3), the maximum beam displacement can be calculated and given by equation (4). The maximum force that the electrothermal actuator can generate is expected to be 45 mN for the chosen dimensions [15]. The maximum beam displacement as a function of beam length is plotted in Figure 2(b). Due to the secant function, the output displacement is expected to be infinite with 2 mm beam length. But, this doesn't occur, because buckling occurs prior to this deformation.

Based on the equations described above, four design parameters were selected and listed in the table 1. The beam width is set to be 10 % bigger than the beam thickness to avoid any in-plane buckling. Other factors are obtained from similar research [15].

Symbol	Design parameter	Optimized values
W	Beam width	33 μm
n	Notch depth	15 μm
L	Beam length	1000 μm
T	Beam thickness	30 μm

Table 1. The dimensions of the design parameters

3. FINITE ELEMENT ANALYSIS OF THE XY STAGE

Finite element analysis (FEA) is utilized to verify the mechanical properties of the proposed actuator determined at the previous section. For this purpose, one of commercial FEA tools, ANSYS1 with the coupled field or multiphysics option, is utilized. The material properties needed for the simulation are cited from reference [15].

For more reasonable results, a few boundary conditions and assumptions are used; (1) the electric input voltage is applied at the two ends of the proposed actuator, (2) both ends of the proposed actuator are assumed to be firmly fixed at the substrate and all the other components are set free without any constraints, (3) one end is electrically isolated from the other, (4) to solve the thermal analysis problem both ends of the proposed actuator areconnected to heat sinks, (5) natural convection or radiation heat transfer are not included in this analysis. .

In the FEA process, a total of 12,650 nodes are generated for the proposed model and occupy 195.7 MB memory. The results from this analysis are described in Figure 3. With a driving voltage of 5.4 V a 2.54 μm displacement is expected along the out-of-plane direction. This displacement generates a maximum of 899.4 MPa von Mises stress and 541.34℃, which is still under its failure strength of 7 GPa (see Figure 3(b)) and its maximum allowable temperature limit of 550 ℃ (see Figure 3(c)). The notches experience of the highest stresses based on this analysis. With these features, the frequency response of the proposed actuator was also checked. Figure 3(d) shows its first resonance mode from the modal analysis. This mode is expected to occur along the out-of-plane direction at 70.4 kHz. The second mode is related to in-plane deformation at 97.6 kHz.

4. MICRO-FABRICATION

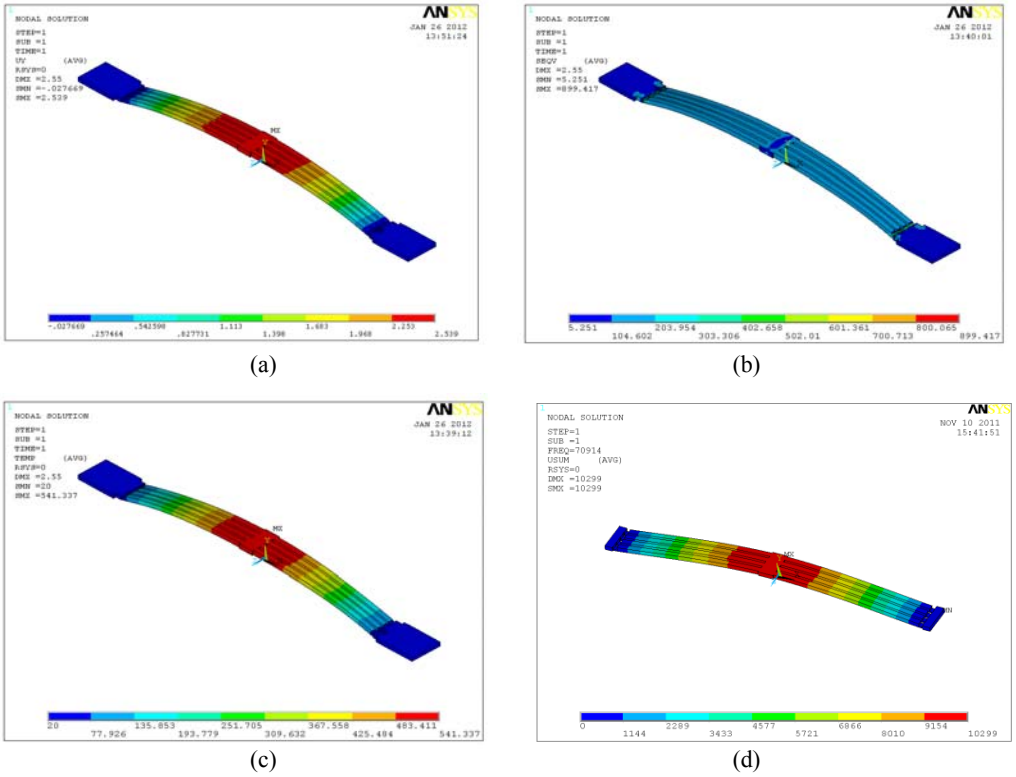

Figure 3. Mechanical properties based on a FEA model; (a) The expected out-of-plane motion; (b) Von Mises stress distribution; (c) temperature distribution; (d) 1st resonant mode

The fabrication process for the proposed out-of-plane actuator is described in Figure 4. The fabrication process is based on the standard SOI MUMPs [15], but additional etching is required for the notches. The starting material is an SOI wafer, with a 30 µm thick device layer, one 2 µm thick buried oxide layer and one 400 µm thick handle layer, as shown in Figure 4(a). The fabrication process consists of four steps; one deposition and three etching steps. The deposition is for electrical connection to the proposed actuators; one layer is a 10 nm of chrome for adhesion and the other layer is 100 nm of gold for wire-bonding and against oxidation. The lithography of this deposition is implemented by a lift-off method and an electron-beam evaporator (Denton Infinity 221). The three etching steps are for the fabrication of the deep Si-trenches and implemented by the Bosch1 process (Deep RIE-Unaxis SHUTTLELINE DSEII1). The first etching is for the notches only (Figure 4(c)) and the second etching is for the main devices including the actuators (Figure 4(d)). Due to the etching depth difference, the notches are separately fabricated from the main devices. Following these steps, the fabrication of the device layer can be completed and the actuator should be released for its operation. For releasing, the handle layer of the SOI wafer was selectively etched away which is the third etching and is shown in Figure 7(e). The final step is to remove the buried oxide layer between the device layer and the handle layer. This layer can be selectively etched away by chemical buffered oxide etchant (B.O.E.) (Figure 7(f)). After the completion of these processes, the proposed actuator can generate the desired motion when a voltage difference is applied to the deposited metal pads.

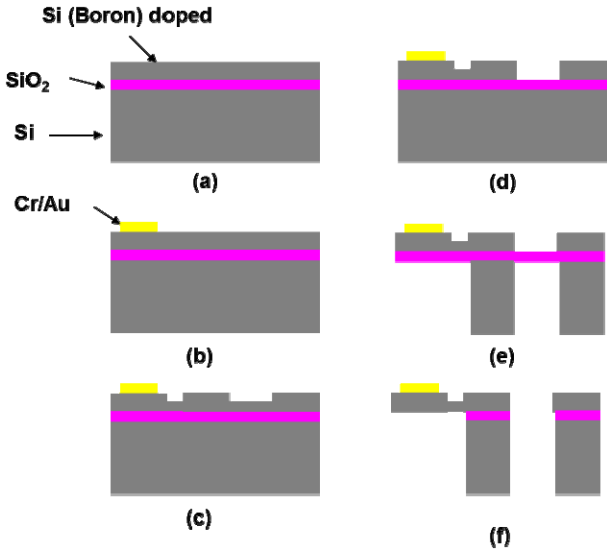

Figure 4. Fabrication sequence: (a) clean SOI wafer as a starting material; (b) metal deposition for electrical connection; (c) etching of the notches on the device layer; (d) etching of the main devices on the device layer; (e) etching of the handle layer to open the bottom side of the devices; (f) removal of the buried oxide layer to release the proposed actuator for its operation

5. TESTING RESULTS

Testing of the proposed actuator, included the measurement of the range of motion and its deformed profiles. An Agilent1 power

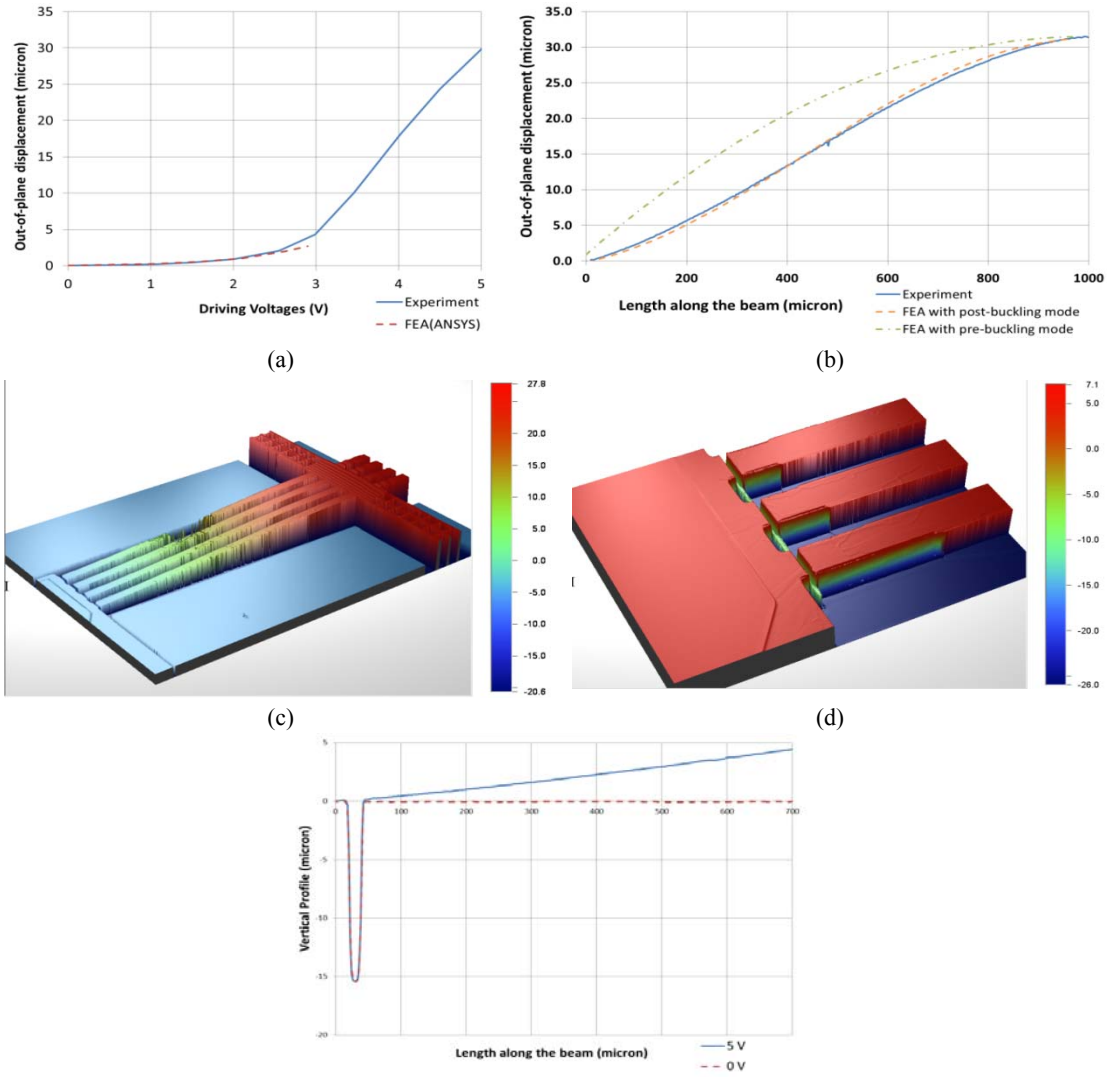

Figure 5. Mechanical behavior of the proposed out-of-plane actuator: (a) relationship between driving voltage and the displacement; (b) measured vertical profile and the expected profile from FEA; (c) 3D scanned image of the half of the actuator (in μm); (d) the 3D scanned imaged on the notch(in μm); (e) the deformation profile near the notch during operation

supply 3322A is utilized to drive the proposed actuator. The mechanical behavior of the proposed actuator is measured with the VEECO1 optical profiler WYKO1 NT1100, which is capable of measuring vertical axis motion with less than 0.1 nm resolution and 1 mm measurement range. The range of motion is measured by controlling the driving current at the power supply from zero to 120 mA for every one voltage difference. After several experiments it was determined that 120 mA is the maximum allowable current that the actuator can endure. The relative position between the two ends of the actuator to the shaft connecting the beams is measured to obtain its displacement, since the maximum displacement is expected to occur at the shaft due to the structure symmetry.

The out-of-plane displacement is measured and plotted in solid line at Figure 5(a). This result is compared with the FEA results plotted with a dotted line. The FEA without the buckling assumption predicts the behavior of the proposed actuator accurately for less than 3 V driving voltage. The relationship between the driving voltage and its corresponding out-of-plane motion in this range is similar with the pattern obtained from the in-plane bent-beam type electrothermal actuator [15]. This is verifying that the same Joule heating and thermal expansion principle apply for their actuations.

For higher than 3 V driving voltage, the actuator starts buckling and its displacement accelerates as shown in Figure 5(a). Due to the buckling, this behavior shows a different pattern of movement from the FEA prediction. Figure 5(b) shows three plots; the experimentally measured deformation profile for 5 driving voltages, the FEA result for pre-buckling mode and the FEA result for post-buckling mode. As buckling occurs near 3 V, the measured profile is similar with the profile for post-buckling mode, not the one for pre-buckling mode. The proposed actuator utilizes both pre-buckling and post-buckling for its operation.

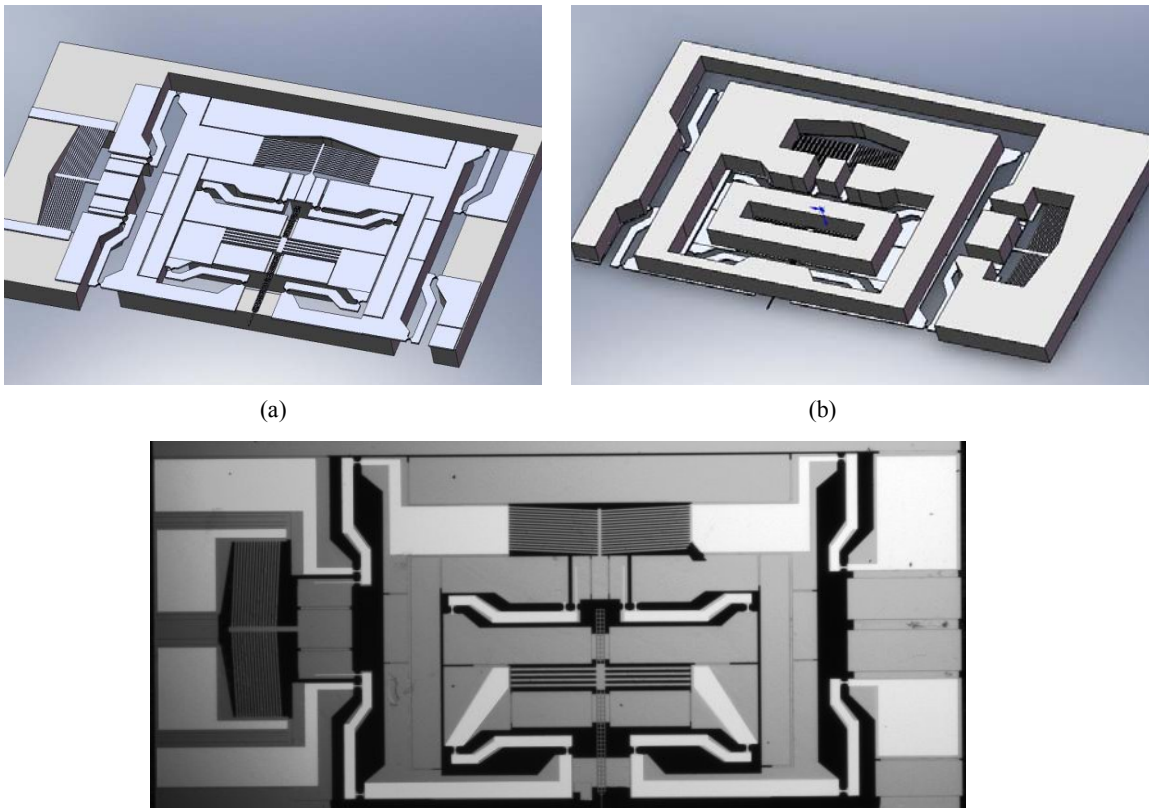

(a) (b)

(c)

Figure 6. A MEMS XYZ stage design with the out-of-plane actuator: (a) angled view of CAD model; (b) a schematic diagram; (c) the fabricated MEMS XYZ stage sample)

Figures 5(c) and 5(d) show the 3-dimensional (3D) images of one-half of the actuator and its notches. Figure 5(e) illustrates the deformation profile near the notch for 5 V driving voltages, when it is in operation and not in operation. The notch gap doesn't change that much during these operations.

6. INTEGRATION WITH THE EXSITING MEMS XY STAGE

To verify the integration capability of the actuator it was embedded into an existing MEMS XY stages whose fabrication process follows the standard SOI-MUMPs, since in this case, significant change in the fabrication process is not needed. The selected MEMS XY stage adopts a serial kinematic mechanism for its operation [15]. By utilizing the serial kinematic mechanism, the proposed single-layer out-of-plane actuator is successfully embedded into the moving platform of the MEMS XY stage. By embedding this out-of-plane actuator, the combined system can generate 3 degrees of freedom (D.O.F.) translational motions along X, Y and Z axes. The detail design of the MEMS XYZ stage is described in Figures 6(a) and 6(b). The in-plane X axis motion is generated by the outer electrothermal actuator and four levers. The moving platform actuated by the outer electrothermal actuator contains the stage aligned along the Y axis. This stage also has one moving platform where the proposed actuator is embedded for the out-of-plane motion or Z axis motion. With this serial kinematic mechanism or dual nested structure, the XYZ stage is implemented without serious coupled motion between them.

Figure 6(c) shows the fabricated sample of the MEMS XYZ stage. The bright white areas indicate the metal deposition for electric connection to the three electrothermal actuators. Greyed area is made of silicon or the device layer of the SOI wafer. Dark black areas are empty area to release the moving platforms and to allow them to move along the designated directions. With a series of experiments, this XYZ stage shows it can generate 40 μm x 40 μm x 30 μm along X, Y and Z axes, respectively.

7. CONCLUSION

This paper describes the design, fabrication and testing of the single layer out-of-plane electrothermal actuator based on MEMS. This actuator is designed to generate out-of-plane motion and the fabricated devices also demonstrate near 32 μm displacements with driving voltage 5 V. Its first resonance mode is expected to occur around 70.4 kHz from FEA. The desired motion is implemented by adopting the notches near its anchors. Joule heating is utilized to generate the thermal expansion of the beam in the actuator, which converts into an eccentric load due to the notches near the beam ends. This eccentric load causes bending of the beams, which transforms into the out-of-plane motion. Due to its simple structure, the fabrication process for the proposed actuator is possible by exploiting the standard SOI-MUMPs. This simple structure also provides good integration capability with other existing MEMS systems which are also based on the SOI-MUMPs. For demonstration, one MEMS XYZ stage is fabricated and tested by embedding the proposed actuator into an existing MEMS XY stage. With this MEMS XYZ stage, 40 μm x 40 μm x 30 μm displacements are measured along each axis without any significant coupled motion error.

8. ACKNOWLEDGMENTS

This research was performed in part in the NIST Center for Nanoscale Science and Technology Nano Fabrication Clean Room. This work was supported by the Measurement Science for Intelligent Manufacturing Robotics and Automation Program of the Intelligent System Division, Engineering Laboratory, National Institute of Standards and Technology, USA.

9. REFERENCES

[1] Du E, Cui H and Zhu Z 2006 Review of nanomanipulators for nanomanufacturing Int. J. Nanomanufacturing 1 (1) 83-104

[2] W. P. Sassen, V.A. Henneken, M. Tichem, P. M. Sarro, "An improved in-plane thermal folded V-beam actuator for optical fibre alignment," J. Micromech. Microeng. 18 (2008) 075033

[3] S. Kwon and L. P. Lee, "Stacked two dimensional micro-lens scanner for micro confocal imaging array," Proc. Fifteenth IEEE International Conference on Micro Electro Mechanical Systems, Las Vegas, NV, USA 20-24 Jan. 2002, pp. 483-486, 2002

[4] Toshiyoshi H, Su G J, LaCosse J and Wu M C 2003 "A surface micromachined optical scanner array using photoresist lenses frabricated by atheraml reflow process" J. Lightwave Technol. 21 1700–8

[5] Kim, K., Liu, X., Zhang, Y., and Sun, Y., 2008, "Nanonewton Force-Controlled Manipulation of Biological Cells Using a Monolithic MEMS Microgripper With Two-Axis Force Feedback," J. Micromech. Microeng., 18 5 ,p. 055013.

[6] Kim C. H., Jeong H M, Jeon J U and Kim Y K 2003 Silicon micro XY-stage with a large area shuttle and no-etching holes for SPM-based data storage J. Microelectromech. Syst. 12 470-8

[7] B. Sahu, C. R. Taylor "Emerging Challenges of Microactuators for Nanoscale Positioning, Assembly, and Manipulation," J. of Manufacturing Science and Engineering, June 2010, vol. 132/030917-1

[8] Bell, D. J., Lu, T. J., Fleck, N. A., and Spearing, S. M., 2005, "MEMS Actuators and Sensors: Observations on Their Performance and Selection for Purpose," J. Micromech. Microeng., 15(7), pp. S153–S164.

[9] J. H. Comtois and V. M. Bright, "Surface micromachined polysilicon thermal actuator arrays and applications," in Proc. Tech. Dig. Solid-State Sens. Actuators Workshop, Hilton Head Island, SC, Jun. 2-6, 1996, pp. 174-176

[10] W. C. Chen, P. I. Yeh, C. F. Hu and W. Fang, "Design and Characterization of Single-Layer Step-Bridge Structure for Out-of-Plane Thermal Actuator," J. of MEMS, Vol. 17, No. 1, Feb. 2008, p70 – p77

[11] M. McCarthy, N. Tiliakos, V. Modi, L. G. Frechette, "Thermal buckling of eccentric microfabricated nickel beams as temperature regulated nonlinear actuators for flow control," Sensors and Actuators A: Physical Volume 134, Issue 1, 28 February 2007, Pages 37-46 International Mechanical Engineering congress and Exposition 2005

[12] J. H. Comtois, V.M. Bright, "Applications for surface-micromachined polysilicon thermal actuators and arrays," Sensor and Actuators A 58, 1997, p19-25

[13] D. M. Burn, V. M. Bright, "Design and performance of a double hot arm polysilicon thermal actuator," proc. Of the SPIE micromachining and microfabrication conference, Austin, TX, Sep. 1997, pp.296-306

[14] F. P. Beer and E. R. Johnston, Jr, "Mechanics of Materials," 2nd edition, McGrawHill, 1992, pp 650 - 653

[15] [Kim YS, Nicholas NG, Gupta SK 2011 A Two Degree of Freedom Nanopositioner with Electrothermal Actuator for Decoupled Motion, ASME/IDETC conference, DC, USA